Hyaluronic acid-bearing lipoplexes: physico-chemical characterization and in vitro targeting of the CD44 receptor

Hyaluronic acid-bearing lipoplexes: Physico-chemical characterization and in vitro targeting of the CD44 receptor

Amélie Dufaÿ Wojcicki[a, b], Hervé Hillaireau[a, b], Thais Leite Nascimento[a, b], Silvia Arpicco[c], Myriam Taverna[a, b], Sandy Ribes[a, d], Mickaël Bourge[e], Valérie Nicolas[a, f], Amélie Bochot[a, b], Christine Vauthier[a, b], Nicolas Tsapis[a, b], Elias Fattal[a, b, ,

[a] Univ Paris-Sud, Faculté de Pharmacie, 5, rue J.B. Clément, 92296 Châtenay-Malabry Cedex, France

[b] CNRS UMR 8612, Institut Galien Paris-Sud, 5, rue J.B. Clément, 92296 Châtenay-Malabry Cedex, France

[c] Università degli Studi di Torino, Facoltà di Farmacia, Dipartemento di Scienza e Tecnologia del Farmaco, Via Pietro Giuria 9, 10125 Torino, Italy

[d] EA4123, 5, rue J.B. Clément, 92296 Châtenay-Malabry Cedex, France

[e] Pôle de Biologie Cellulaire, Imagif, Centre de recherche de Gif, (FRC3115), CNRS, IFR87, 91198, Gif-sur-Yvette Cedex, France

[f] IFR 141-IPSIT Microscopy facility, 5, rue J.B. Clément, 92296 Châtenay-Malabry Cedex, France

Elias Fattal Corresponding author at: Université de Paris Sud 11, UMR CNRS 8612, Institut Galien Paris-Sud, Faculté de Pharmacie, 5 rue JB Clément, F-92296 Châtenay-Malabry, France. Fax: + 33 146835946.

elias.fattal@u-psud.fr

Abstract

The mechanism by which hyaluronic acid (HA)-bearing lipoplexes target the A549 lung cancer cell line was evaluated. For this purpose, cationic liposomes targeting the CD44 receptor were designed thanks to the incorporation in their composition of a conjugate between high molecular weight HA and the lipid DOPE (HA-DOPE). Liposomes containing HA-DOPE were complexed at different lipids:DNA ratios with a reporter plasmid encoding the green fluorescent protein (GFP). Diameter, zeta potential, lipoplex stability and DNA protection from nucleases have been determined. Lipids:DNA ratios of 2, 4 and 6 provided a diameter around 250 nm with a zeta potential of – 30 mV. The strength of lipids:DNA interaction and the fraction of DNA protected from enzymatic degradation increased with the lipids:DNA ratio. 2D-immunoelectrophoresis demonstrated the low capacity to activate the C3 fraction of the complement system of any of these three ratios, with and without HA-DOPE. Transfection efficiency in the presence of 0, 10 and 15% of HA-DOPE or unconjugated HA, was determined on the CD44-expressing A549 cells by flow cytometry. Lipoplexes at a lipids:DNA ratio of 2 containing 10% (w/w) of HA-DOPE were the most efficient for transfection. The maximal level of GFP expression was obtained after 6 h of incubation demonstrating a slow transfection kinetics of lipoplexes. Finally, lipoplex cellular uptake, measured indirectly by the level of transfection using flow cytometry and validated by fluorescence microscopy, was shown to be mediated by the CD44 receptor and caveolae. These results demonstrate the strong specificity of DNA targeting through the CD44 receptor using HA of high molecular weight as a ligand.

Keywords

Lipoplexes; Hyaluronic acid; A549; CD44; Endocytosis; Complement activation

1. Introduction

Designing non-viral gene delivery systems has been over the last two decades an important research area aiming to improve both stability and efficiency of the delivered plasmid DNA [1]. Development of carriers mediating safe and efficient gene transfer has been required to reach therapeutic levels of protein expression. In such context, synthetic vectors have emerged as an attractive strategy as they are able to protect DNA from nuclease degradation and to induce its condensation therefore reducing its size and making their cell uptake possible. Among the non-viral gene delivery systems, cationic liposomes have been widely investigated. Their main advantages include low immunogenicity [2] and toxicity [3] and [4] as compared to viral vectors [5] and [6] and their potential to transfect diverse tissues and cell types [4], [5], [6] and [7]. Nevertheless, several observations have limited the use in clinics of cationic lipid delivery systems. At first, it was observed *in vivo* in animal models that they aggregate in serum and therefore, accumulate in organs of the mononuclear phagocyte system (MPS), being taken up by macrophages [8]. When covering lipoplexes by polyethyleneglycol (PEG) to reduce opsonisation and MPS uptake, a decrease of transfection efficiency was observed *in vitro* [9] and [10]. Moreover, it was shown that the use of PEG combined with liposomal formulations containing DNA makes them less efficient *in vitro* [9] and more immunogenic [11].

Hyaluronic acid (HA) is a glycosaminoglycan composed of non-esterified disaccharidic units of *N*-acetylglucosamine and glucuronic acid chains alternately β1→4 and β1→3. It is the major component of the extracellular matrix, being therefore ubiquitous. Contrary to HA oligomers, the native high molecular weight HA does not induce expression of genes involved in proliferation or inflammation [12] and counteracts proangiogenic effects of the oligomers [13]. Even if native HA can activate some signaling pathways, this occurs at levels far lower than with HA oligomers [12]. All this has led to consider the high molecular weight HA as a “bioinert” component [14]. Most interestingly, HA was proposed as an alternative to PEG, to target liposomes encapsulating small molecules [15] and [16] or lipoplexes [17]. HA presents two advantages. First it can be an addressing molecule due to the expression of its membrane receptor, CD44, on tumor initiating cells (TIC) [18] and second because it is a hydrophilic polymer, it could prevent opsonin adsorption by steric repulsion allowing to reduce MPS uptake.

We have synthesized a HA-DOPE conjugate which was included in lipoplexes demonstrating an improved transfection of breast cancer cells when these cells express the CD44 receptor [17]. These first results have demonstrated that using HA was indeed relevant for increasing the expression of a reporter gene in a cancer cell line. However, the extent of HA anchoring to lipoplexes and the

mechanism of uptake remained open questions. The present report aims to produce the evidence of the presence of HA on lipoplex surface and clarify their mechanism of internalization through their interaction with the CD44 receptor on the A549 lung cancer cell line.

2. Materials and methods

2.1. Materials

High molecular weight hyaluronic acid (HA) (sodium salt, 1600 kDa, purity of 95%) was purchased from Acros organics (Geel, Belgium). L-alpha-dioleylphosphatidylethanolamine (DOPE) and phosphatidylethanolamine conjugated to rhodamine (PE-rhodamine) were provided by Avanti Polar Lipids distributed by Sigma Aldrich (Saint Quentin Fallavier, France). The cationic lipid [2-(2-3didodecyloxypropyl)hydroxyethyl]ammonium bromide (DE) was synthesized as described [19]. Capillary electrophoresis of the conjugate shows that all DOPE molecules were linked to HA and that there was no free HA in the mixture. Research grade plasmid pCMV-GFP pF463 (3487 bp) was purchased from Plasmid factory (Bielefeld, Germany).

2.2. Lipoplex preparation

To prepare liposomes, a thin lipid film was obtained by evaporation under vacuum of a chloroformic solution of an equal mixture (w/w) of DE and DOPE using a rotative evaporator. The lipid film was then hydrated with an aqueous solution of 10% (w/v) HA-DOPE conjugate at a final concentration of 1 mg/mL during 8 min under vortex stirring until complete film detachment and formation of a liposomal suspension. Various volumes of liposomal suspension were gently added to a 1 mg/mL pCMV-GFP solution at different lipids:DNA ratios. Complexation under nitrogen, at ambient temperature, was carried out during at least 1 h before use. Fluorescently labeled lipoplexes were prepared similarly by substituting 6% (w/w) of DOPE by PE-rhodamine.

2.3. Differential scanning calorimetry

Differential scanning calorimetry (DSC) analysis was performed on hydrated samples using a differential scanning calorimeter (DSC 7, Perkin Elmer, USA) equipped with the Pyris software. 12 h before the experiment, lipid films of DOPE (10 mg) were hydrated either with 100 µL MilliQ water or with 100 µL of a 10 mg/mL HA-DOPE solution. Then about 4 mg of accurately weighted samples were introduced into a 40 µL pan and analyzed. DSC runs were conducted from − 40 °C to + 90 °C

at a rate of 10 °C/min. Calibration was achieved using n-decane (T_m = − 28.11 °C) as well as indium (T_m = 156.83 °C). Enthalpies were normalized with respect to DOPE weight in the sample.

2.4. Capillary electrophoresis

A Beckman P/ACE System 5500 was used with an uncoated fused silica capillary (length to detector: 57 cm and internal diameter: 75 µm) on normal polarity. Electrophoresis conditions to analyze HA-DOPE conjugate were derived from Grimshaw et al. for the assay of HA [20]. The capillary was first conditioned by 4 successive rinsings for 5 min each with water, 1 M NaOH, 0.1 M NaOH and back to water. Then before each analysis, the capillary was washed with successively (and at 20 psi), water for 1 min, 0.1 M NaOH for 2 min, water for 1 min, 0.1 M HCl for 2 min, water for 2 min and finally equilibrated with the background electrolyte for 2 min. The separation buffer was 40 mM sodium tetraborate containing 40 mM of sodium dodecyl sulfate (SDS). Sample injection was done under nitrogen at 0.5 psi for 2 s. All samples were adjusted at a concentration of 0.5 mg/mL of HA or HA-DOPE by evaporation under vacuum using an Eppendorf Concentrator® at 30 °C, which concentrated liposomes 5-fold and lipoplexes 8-fold. This step was validated after verification by dynamic light scattering that no modification of the diameter and zeta potential occurred during this concentration step (data not shown). Detection wavelength was 200 nm and the voltage applied was 18 kV. The capillary was maintained at 25 °C during electrophoresis. Experiments were performed at least in duplicate.

2.5. Diameter and zeta potential measurement

Diameter and zeta potential were determined with a Zetasizer Nano Zs (Malvern Instruments Ltd, Malvern, UK). Before each measurement, liposomes and lipoplexes were diluted at 2% (v/v) in 1 mM NaCl. Measurements were carried out in triplicate at 25 °C on three independent preparations. Size measurements were also performed in cell culture media.

2.6. Gel migration assay

After addition of BB5X blue (10 mM Tris pH 7.4, 2 mM EDTA, 25% glycerol, 0.02% bromophenol blue, and 0.02% xylene cyanol), 2 µg of plasmid, free or complexed to liposomes at different lipids:DNA ratios (1, 2, 3, 4, 6, 8) were loaded on a 1% agarose gel in TBE1X buffer (89 mM Tris, 89 mM boric acid, 2 mM EDTA disodium salt) containing ethidium bromide, and migrated at 100 V for 20 min. DNA which was not bound to liposomes migrated under electric field.

2.7. Protection against degradation by nucleases

2 µg of plasmid complexed or not to liposomes at different lipids:DNA ratios (1, 2, 3, 4, 6, 8) were digested by 2 IU of DNase I (Invitrogen, Cergy Pontoise, France) for 30 min at 37 °C in the presence of 20 mM $MgCl_2$. The digestion was stopped by heating the mixture at 60 °C for 10 min in the presence of 50 mM EDTA. Lipids were then solubilized in an SDS solution up to a final detergent concentration of 17 mM. After vigorous agitation, samples were centrifuged at 10,000 rpm for 5 min then heated at 75 °C for 15 min. Each sample was loaded on a 1% agarose gel in TBE 1X as described for gel migration assay.

2.8. Evaluation of activation of C3 protein of the complement system

Conversion of plasmatic C3 protein into C3b and C3a fragments, signing an activation of the complement system, was evaluated by 2-D immunoelectrophoresis using a polyclonal antibody to human C3 as described [21]. Lipoplexes of lipids:DNA ratios of 2, 4 and 6 with or without HA-DOPE were prepared, then concentrated 10-fold at 30 °C using an Eppendorf Concentrator® in order to obtain a sufficient specific surface. Veronal Buffer Saline (VBS) containing 0.15 mM Ca^{2+} and 0.5 mM Mg^{2+} ions (VBS^{2+}) and VBS containing 40 mM ethylenediaminetetraacetic acid (VBS–EDTA) were prepared as described by Kazatchkine et al. [22]. A volume of suspension equivalent to a specific surface of 230 cm^2 (calculated by $Sspecific = \frac{6 \times m}{D \times d}$ Sspecific=6×mD×d where D is the average diameter, m is the mass contained in the sample, and d is the density) was incubated under gentle agitation for 1 h at 37 °C with 50 µL of human serum (EFS Ile-de-France, Kremlin-Bicêtre) and 50 µL of VBS^{2+}. All experiments were done with the same human serum which was tested for functionality prior to be used in the present test. The absence of lipoplex size modification in this medium was checked. Briefly, samples were subjected to a first electrophoresis on 1% agarose gel in tricine buffer, then deposited on a Gelbond® film coated with agarose gel containing a polyclonal antibody to human C3 (Sigma, France) at 0.1 mg/mL. This polyclonal antibody can recognize the native and activated form of the protein C3. The samples were then subjected to a second dimension electrophoresis, followed by protein precipitation and fixation in 0.15 M NaCl and further drying. Films were finally stained with coomassie blue to reveal the presence of native C3, and lower molecular weight active fragments C3a and C3b precipitated with the antibody. Each sample was analyzed three times across the whole process. Activation of the C3 protein was expressed as the complement activation factor (CAF) defined as the ratio of the peak surface of C3a + C3b detected on the plate over the sum of the peaks surface of C3 and C3a + b, using the following equation:

$CAF = \frac{(C3a + C3b)}{C3 + (C3a + C3b)}$CAF=(C3a+C3b)C3+(C3a+C3b). Areas under the peaks were measured using ImageJ software.

2.9. Cell culture

Human lung cancer A549 cells (ATCC CCL-185) were cultured in Roswell Park Memorial Institute (RPMI) Medium 1640 (Lonza, Belgium) supplemented with 10% fetal bovine serum (FBS, Lonza, Belgium), 50 U.mL^{-1} penicillin, 50 U.mL^{-1} streptomycin and 1% glutamine. Cells were maintained at 37 °C in a humidified atmosphere with 5% CO_2.

2.10. Assessment of CD44 expression

A549 samples for assessment of CD44 expression were prepared as described before [17]. For all flow cytometry experiments, cells were excited at 488 nm with an argon laser source, and emission was analyzed through a 510/20 nm band-pass filter for GFP, a 529/28 nm band-pass filter for FITC. Doublets were eliminated by pulse discrimination. The cytometer was a MoFlo XDP (Beckman Coulter) driven by the Summit software. Analysis was done in duplicate with 10,000 cells measured in each sample. Results are given as a percentage of cells above fluorescence threshold.

2.11. Cell transfection

Cells were seeded in 500 µL of growth medium (7.5×10^4 cells.mL^{-1}) in 24-well plates (TPP, Switzerland) and pre-incubated for 24 h. Just before treatment by various lipoplexes formulations (lipids:DNA ratios of 2, 4 and 6; without or with 10 and 15% of HA-DOPE or unconjugated HA) for 24 h at 10 µg/mL, cells were washed and recovered with medium without serum. Lipofectin®, a formulation of DOTMA:DOPE (1:1), was used as a positive control. Cells were washed and medium with FBS was introduced 24 h after transfection. To study the transfection kinetics, medium was removed 2, 6 or 24 h after the beginning of the treatment by lipoplexes of ratio 2 with 10% HA-DOPE. Medium containing FBS was added 24 h after transfection. Samples were prepared 54 h after transfection for flow cytometry experiments. After detachment, cells were washed by PBS and then recovered in 600 µL of 1% paraformaldehyde in PBS at 4 °C. Analyses were achieved by flow cytometry as described for assessment of CD44 expression. 5000 cells were measured per sample and each analysis was done in triplicate. The normalized transfection efficacy index (NTEI) was calculated according to the following equation:

$$NTEI = \%\ of\ singulet\ living\ cells\ which\ express\ GFP \times \frac{fluorescence\ intensity\ of\ GFP^{+}\ cells}{fluorescence\ intensity\ of\ GFP^{-}\ cells}$$

NTEI=%ofsinguletlivingcellswhichexpressGFP×fluorescenceintensityofGFP+cellsfluorescenceintensityofGFP−cells

Turn MathJax on

Moreover, results of kinetics study expressed in NTEI are also presented in percentage, taking into account that the value of NTEI at 24 h is fixed at 100%.

2.12. Endocytosis pathways

The concentrations of the endocytic inhibitors were set after the following optimization. Each inhibitor was incubated at various concentrations (1, 6, 15, 25, 50 μM chlorpromazine; 1, 4, 7 μM filipin; 50, 75, 100, 200 μM genistein; 2–7 mM methylβcyclodextrin; 0.5, 1.6, 2, 10 μg/mL CD44 antibody) and the cell viability was monitored by flow cytometry. The maximal concentration associated to absence of toxicity was then selected for each inhibitor, except for methylβcyclodextrin which was found toxic at all tested concentrations.

A549 cells were pretreated with aqueous solutions of 1 μM chlorpromazine, high molecular weight HA in 50-fold the amount contained in lipoplexes 10% HA, 1.6 μg/mL CD44 antibody (clone A3D8), 50 μM genistein, 1 μM filipin (Sigma Aldrich, France) (a control experiment was performed including the same volume of ethanol than what is contained in filipin solution). After 1 h of incubation at 37 °C in a humidified atmosphere with 5% CO_2 (except 2 h for CD44 antibody), lipoplexes of ratio 2 with 10% HA-DOPE were added (10 μg/mL). Medium was removed after 6 h. Medium containing FBS was added 24 h after transfection. Samples for flow cytometry analysis were prepared as previously described for study of cell transfection 54 h after transfection. Results expressed in NTEI are presented in percentage, taking as reference for 100%, the NTEI of control without inhibitory treatment. These studies were coupled with fluorescence microscopy. *In vitro* imaging acquisition was performed with a Zeiss videomicroscope (Axio Observer Z1) equipped with an incubator (temperature and CO_2 controlled) in order to collect the green fluorescence on living cells. All images were acquired with a 20 ×/0.8 plan-Apochromat objective lens using a 470 nm LED for excitation and a 505–550 nm band pass filter to quantify the emission of fluorescence. Videomicroscope was coupled with a MRm CCD camera.

2.13. Intracellular trafficking

The uptake and intracellular trafficking of lipoplexes (at a lipids:DNA ratio of 2 with 10% HA-DOPE) was investigated on A549 cells using confocal laser scanning microscopy. A549 cells were seeded at 35,000 cells/cm^2 on coverslips and cultured for 24 h at 37 °C, 5% CO2. The cells were then treated with fluorescent lipoplexes at the final concentration of 10 µg/mL. After 2 h, 6 h or 24 h incubation cells were rinsed with PBS and fixed by addition of 800 µL of 4% paraformaldehyde in PBS (w/v) during 20 min. After washing with PBS, 10 µL of Vectashield® mounting medium for fluorescence (Vector Laboratories, Inc., Burlingame, CA, USA) was used to prepare the slides. Fluorescence experiments were performed with a confocal laser scanning microscope LSM 510-Meta (Zeiss, Germany) using a 63 ×/1.4 plan-Apochromat objective lens, a helium neon laser (excitation wavelength 543 nm) and a long pass emission filter LP 560 nm. The pinhole was set at 1.0 Airy unit (0.8 µm optical slice thickness). 12 bit numerical images were acquired with LSM 510 software version 3.2. Red intensity profiles were plot with Image J (version 1.42) software (NIH, USA) and the 3D reconstructions and surface rendering were generated using IMARIS 7.1.1 (Bitplane, Zurich) imaging software.

3. Results

3.1. Characterization of HA-DOPE lipoplexes

The physico-chemical studies aimed to evaluate the presence of the conjugate within liposome structure. Differential scanning calorimetry analysis of DOPE demonstrated that the endotherm of gel to liquid crystal phase transition shifted from – 10.30 °C with water or unconjugated HA to – 8.97 °C with HA-DOPE (Supplementary Fig. S1). Assessment of the HA-DOPE purity and determination of the HA fraction bound to liposomes or lipoplexes were carried out by capillary electrophoresis by determination of the free fraction of HA (Fig. 1).

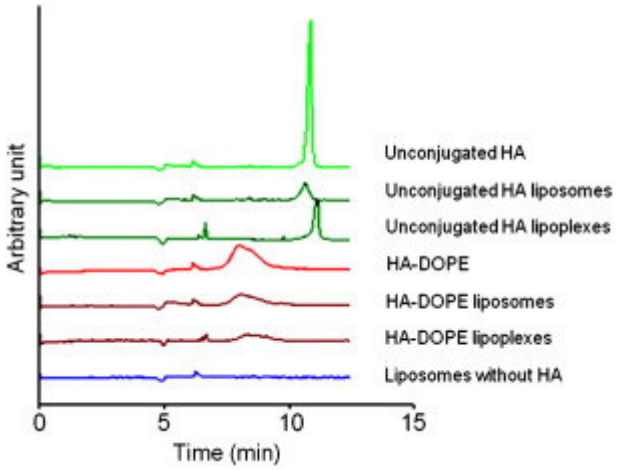

Fig. 1.

Electropherogramms obtained by capillary electrophoresis of 0.5 mg/mL unconjugated HA, 0.5 mg/mL HA-DOPE, liposomes with unconjugated HA or HA-DOPE or without any HA, lipoplexes with unconjugated HA or HA-DOPE.

HA-DOPE migration time was 9 min and the electrophoretic profile did not display the characteristic peak of unconjugated HA which appears at 12 min, demonstrating the absence of free HA in the conjugate. 80 ± 3.1% of unconjugated HA is bound to liposomes, but after DNA addition only 17 ± 1.3% remains associated to them. However in the case of HA-DOPE, only 61 ± 1.0% of HA-DOPE is associated to liposomes, but 42 ± 10.7% remains associated after lipoplex formation. Whereas the liposome diameter was similar at around 400 nm with or without HA, significant reduction of the zeta potential was observed when liposomes are associated to 10% of HA-DOPE or unconjugated HA compared to plain liposomes ($p < 0.0001$) (Fig. 2).

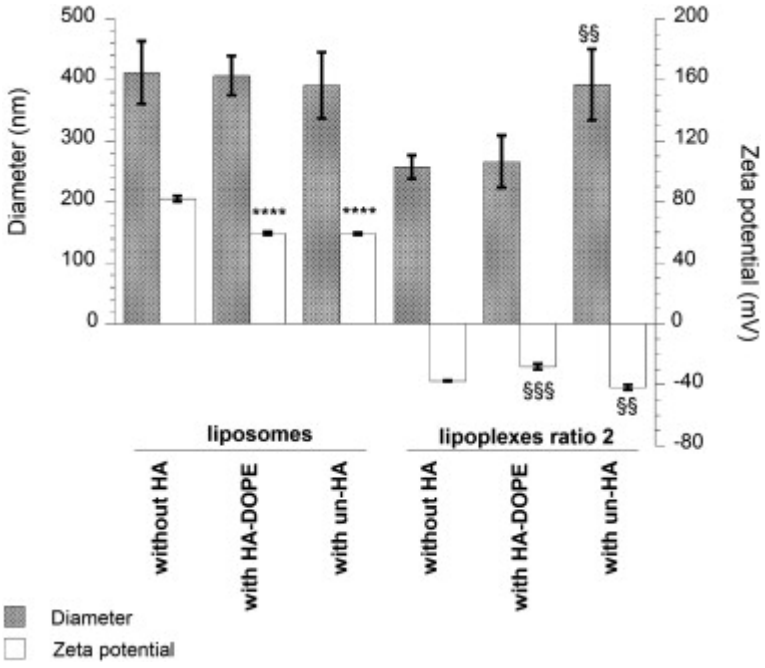

Fig. 2.

Diameters and zeta potentials of liposomes, compared to lipoplexes at a lipids:DNA ratio of 2 containing or not 10% HA-DOPE or unconjugated HA (un-HA) (*vs*. liposomes without HA: **** $p < 0.0001$; *vs*. lipoplexes without HA: §§ $p < 0.01$; §§§ $p < 0.001$) (n = 3).

Addition of DNA to liposomes decreased their diameter in the same way for lipoplexes formulations without HA or with 10% HA-DOPE, but not for lipoplexes with 10% unconjugated HA. Presence of DNA lowers zeta potential values to around − 30 mV. Finally, the diameter and zeta potential values

were similar between lipids:DNA ratios varying from 1 to 6 in presence of HA-DOPE, being around 300 nm and − 30 mV (Fig. 3).

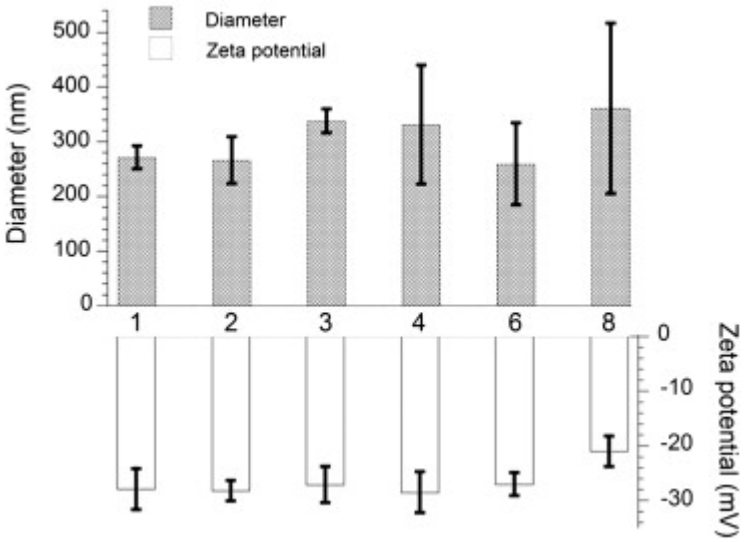

Fig. 3.

Diameters and zeta potentials of lipoplexes at different lipids:DNA ratios (1, 2, 3, 4, 6, 8) (n = 3 on 3 independent preparations).

For the highest lipids:DNA ratio tested, 8, the diameter and the zeta potential increased respectively to values of 361 ± 156 nm and − 21.0 ± 2.7 mV.

3.2. DNA stability and DNA–liposome interactions

Assessment of the interaction between DNA and liposomes was carried out by electrophoresis on agarose gel (Fig. 4).

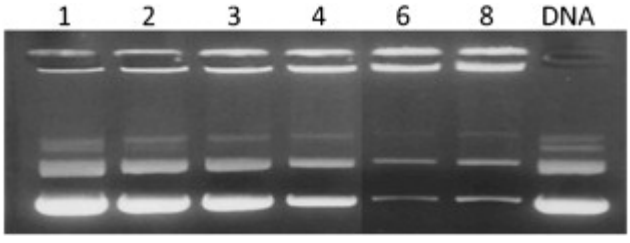

Fig. 4.

1% agarose gel showing profile migration of plasmid in lipoplexes at different lipids:DNA ratios (1, 2, 3, 4, 6, 8) with 10% HA-DOPE, at a constant amount of DNA and comparison with free DNA. The non-migrating plasmid is on the top of the gel image. DNA bands on the bottom are the fraction of DNA that can be separated from the lipoplexes by electrophoresis.

DNA migration shows that when the lipids:DNA ratio increased, the associated fraction increased and the quantity of free or weakly associated fractions was reduced. A similar experiment was carried out after incubation of lipoplexes with DNAse I (Fig. 5).

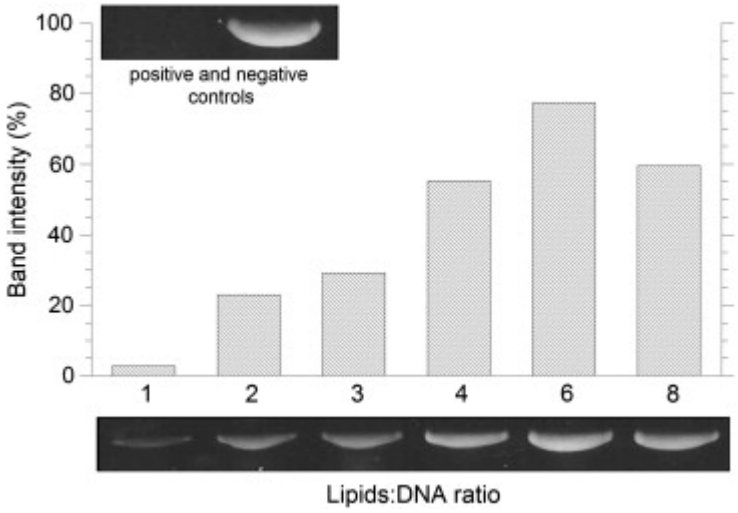

Fig. 5.

1% agarose gel showing migration profile of plasmid in lipoplexes for different lipids:DNA ratios (1, 2, 3, 4, 6, 8) with 10% HA-DOPE at constant amount of DNA after DNAse I exposition (in unit sufficient to total digestion as shown by positive control). Histograms present band intensity determined thanks to ImageJ software (% compared to the negative control set at 100%).

This experiment demonstrates that the more the cationic lipids, the better the protection against DNAse I is. Indeed protection increased from 3% to 77% with lipids:DNA ratios varying respectively from 1 to 6. The protection effect then decreased slightly, being 60% for a lipids:DNA ratio of 8.

Noteworthy, the diameter of lipoplexes evaluated on cells in the following (lipids:DNA ratio of 2, 10% HA-DOPE) did not differ significantly in the serum-containing cell culture media (249 ± 27 nm).

3.3. Evaluation of the activation of the C3 protein of the complement system

Complement activation was determined by 2D-immunoelectrophoresis of C3 on lipoplexes made with three lipids:DNA ratios of 2, 4, 6 with or without 10% of HA-DOPE (Fig. 6).

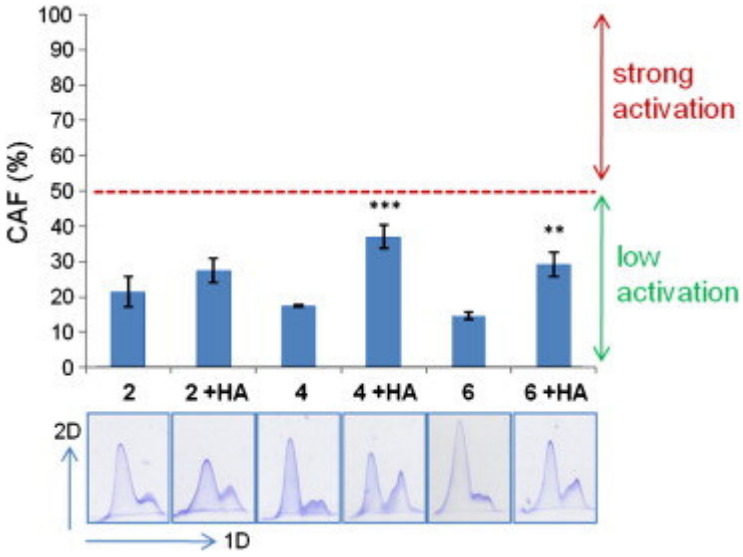

Fig. 6.

Activation factor of the C3 protein (CAF) values for lipoplexes at lipids:DNA ratios of 2, 4, 6, with or without 10% of HA-DOPE, after substraction of the CAF value corresponding to spontaneous activation of serum (100% matches for CAF value of positive controls at the specific area of 230 cm^2) (with HA-DOPE *vs* without HA-DOPE: ** $p < 0.01$; *** $p < 0.001$).

Although lipoplexes containing HA-DOPE with lipids:DNA ratios of 4 and 6 give higher CAF values than the respective samples without HA-DOPE, all formulations tested possess CAF values under 50%, which corresponds to a low activation of the complement (incubation time of 1 h, a specific surface value of 230 cm^2).

3.4. Transfection of CD44-expressing A549 cells

As seen by flow cytometry, 99.98% of A549 cells express CD44 on their surface (Fig. S2). Cell viability measured by MTT was always above 80% for concentration of lipoplexes up to 10 µg/mL in culture medium, independently of lipids:DNA ratio and whether HA-DOPE was present or not in the formulation (data not shown). The percentage of transfected cells reached 17% at 2 h and plateaued at 33% from 6 h (Fig. S3). After 2 and 6 h of incubation with lipoplexes, the NTEI reached respectively 50 and 100% of the maximal level equivalent to the one obtained with 24 h of incubation (Figure S3). Comparison of different lipids:DNA ratios shows that, despite an equivalent amount of intact DNA, the lipids:DNA ratios of 2 and 4 are more effective than 6 (Fig. 7).

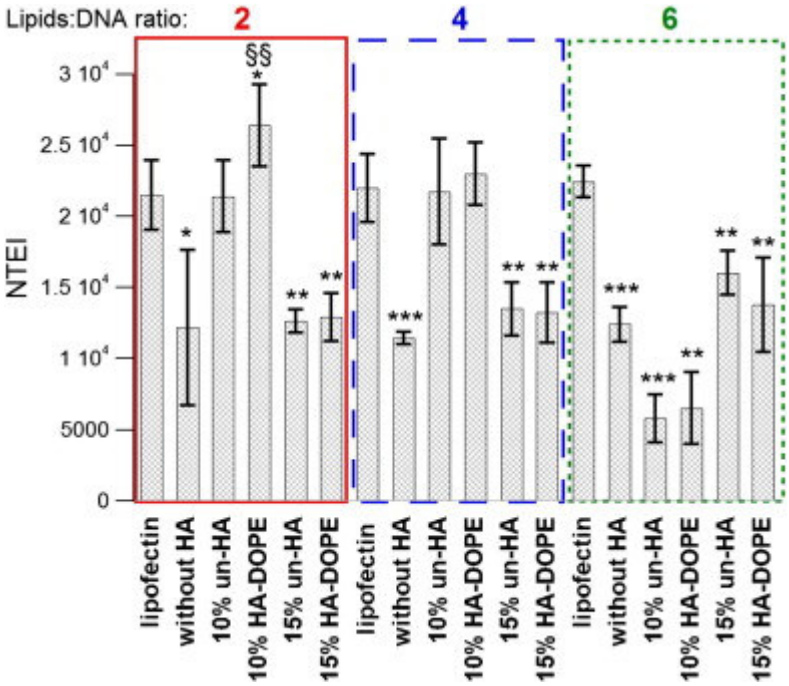

Fig. 7.

Normalized transfection efficacy index (NTEI) of lipoplexes, as a function of the lipids:DNA ratio (2, 4, 6), the mode (conjugated or unconjugated) and the rate (0, 10 or 15%) of HA incorporation, and comparison with Lipofectin® at the same lipids:DNA ratios (2, 4, 6) (*vs* Lipofectin® at same ratio: * $p < 0.05$; ** $p < 0.01$; *** $p < 0.001$; *vs* unconjugated HA at same ratio: §§ $p < 0.01$; n = 3).

For these two more efficient ratios, the addition of 10% HA-DOPE, but not 15%, increased significantly the GFP expression. Lipids:DNA ratio of 4 containing 10% HA-DOPE and unconjugated HA present the same GFP expression levels as Lipofectin®. For the ratio 2 containing 10% of HA, a larger transfection efficiency was observed compared to other treatment and particularly compared to unconjugated HA ($p < 0.01$) and Lipofectin® ($p < 0.05$).

3.5. Determination of endocytosis pathways

Cell treatment with HA 50X, which saturates CD44, or CD44 antibody which blocks the HA receptor, both resulted in a 40% decrease of GFP expression (Fig. 8).

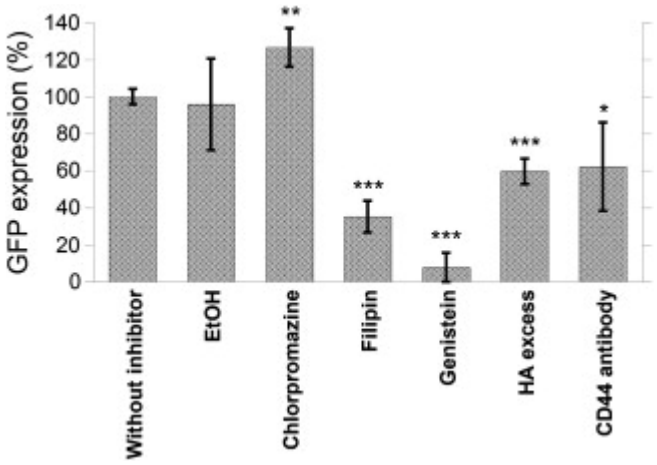

Fig. 8.

Effects of endocytosis-interfering treatments on GFP expression studied by flow cytometry. A549 were incubated for 6 h with lipoplexes with a lipids:DNA ratio of 2 containing 10% of HA-DOPE, 1 h (except 2 h for CD44 antibody) after pretreatment with 1 μM chlorpromazine, 1 μM filipin (+ control ethanol alone), 50 μM genistein, excess of high molecular weight HA (50X), and 10 μg/mL CD44 antibody. NTEI results are expressed in percentage with NTEI of control cells set at 100% (* $p < 0.05$; ** $p < 0.01$; *** $p < 0.001$; n = 3).

Incubation with filipin, an inhibitor of caveolae-mediated endocytosis, reduces the transfection by 60%. Moreover, when genistein, another inhibitor of this internalization pathway, is used, GFP expression is lowered by 90%. In contrast, using chlorpromazine, a clathrin-mediated endocytosis inhibitor, transfection levels were not changed. Microscopy experiments enable to verify visually the cell integrity (no dysmorphy or autofluorescent dead cells) and coincide with flow cytometry results (Supplementary Fig. S4).

3.6. Intracellular trafficking

The uptake and intracellular trafficking of lipoplexes (lipids:DNA ratio of 2, 10% HA-DOPE, containing PE-rhodamine) in A549 cells was assessed on 0.8 μm thick slices by confocal microscopy (Fig. 9, and Supplementary Fig. S5 for 3D reconstructions). The observations (Fig. 9A) and intensity profiles (Fig. 9B) show a progressive uptake of lipoplexes, the global fluorescence increasing from 2 h to 6 h and 24 h incubation. The fluorescence pattern also changes during incubation. After 2 h, cells mostly show a cytoplasmic intense punctuated fluorescence (and a slight diffuse fluorescence), consistent with the presence of endosomal vesicles containing lipoplexes. After 6 h and 24 h, between one third and one half of the cells exhibit intense cytoplasmic diffuse fluorescence, indicating the presence of the fluorescent lipids in the cytosol.

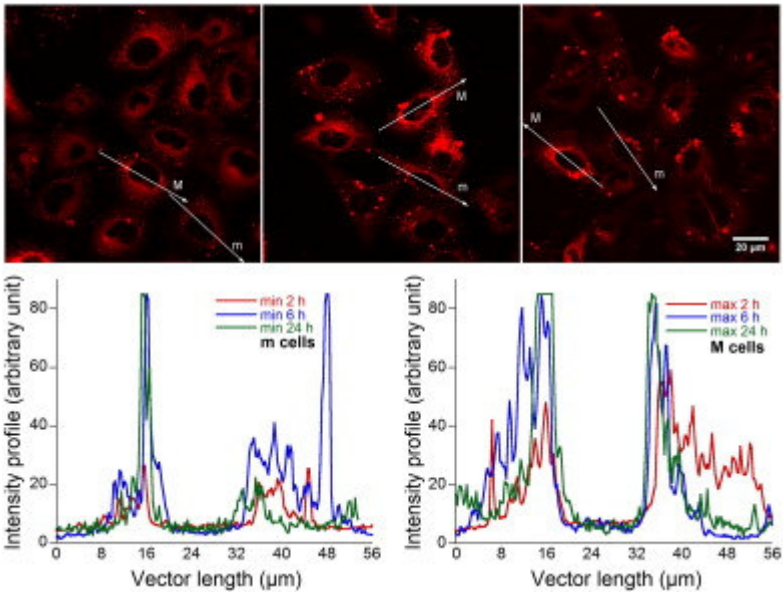

Fig. 9.

A. Uptake and intracellular trafficking of fluorescent lipoplexes (lipids:DNA ratio of 2, 10% HA-DOPE) after 2 h (left), 6 h (middle) and 24 h (right) incubation with A549 cells, as evaluated by confocal laser scanning microscopy. For each images, composed of (z-axis) projection of three median optical slices of 0.8 µm thick, cells with a mininum fluorescence intensity (m) and a maximal fluorescence intensity (M) are shown. B. Red intensity profiles of m and M cells, are respectively presented on the left and right graphs (at 2 h (red), 6 h (blue) and 24 h (green) incubation).

4. Discussion

The present report was aiming to understand the mechanism of interaction of HA-bearing lipoplexes with CD44 receptor-expressing cells. The first underlying basic assumption of our study was that HA-DOPE conjugate could be inserted into vesicle bilayers thanks to its hydrophobic moiety. The HA-DOPE conjugate is obtained through the creation of an amidic bond between the carboxylic group of HA and the amino group of DOPE. However, the affinity between the conjugate and lipids forming the liposome bilayer was questionable regarding the large difference of molecular weight existing between DOPE (740 $g.mol^{-1}$) and HA (1.6×10^6 $g.mol^{-1}$). Differential scanning calorimetry revealed a difference of behavior between unconjugated HA and HA conjugated to DOPE suggesting that DOPE covalently linked to HA interacts with DOPE, being therefore able to play the role of anchor in the lipid membrane.

Previous studies by Surace et al. [17] have shown that 10% HA-DOPE (w/w) was optimal for transfection of MDA-MB231 breast cancer cells expressing CD44. We have therefore used this

amount of conjugate and formulated lipoplexes at different lipids:DNA ratios. Whereas all lipoplex formulations were negatively charged, a reduction of the zeta potential was only seen for the highest lipids:DNA ratio of 8. Nevertheless, at these lipids:DNA ratios, the size distribution was polydisperse. It was shown previously that lipoplex size and heterogeneity of the structures both appear to increase along with the lipids:DNA ratio probably because the density of the complexes decreases as the lipids:DNA ratio increases [23]. Nevertheless, estimation of lipoplex stability by gel migration reveals that the more lipids were introduced to a constant amount of DNA, the stronger the interactions in lipoplexes. At lowest lipids:DNA ratios, the low amount of cationic charges left a large part of DNA free from any interaction. However, capillary electrophoresis shows that there is no migration of free DNA at a ratio of 2 (no peak at 32 min as control DNA alone, data not shown). At high lipids:DNA ratios of 6 or 8, the amount of free DNA was low meaning that all charges from DNA are involved in the interaction with cationic liposomes. These data are of high interest since even with a high amount of cationic lipids, the particles remain negatively charged. Cationic charges are known to promote strong instabilities in the presence of serum leading to aggregation [24]. This phenomena would disappear in presence of the lipoplexes designed here. Finally, as the amount of cationic lipids increases, an increase of the protection ability against DNAse I is observed with a maximum of protection close to 80% for a lipids:DNA ratio of 6. This protection then decreases at the ratio of 8 where the density of the lipoplexes is supposed to be lower (as shown by size measurements), allowing more access to the degrading enzymes. In relation to these data, the lipoplex formulations of ratios 2, 4 and 6 were considered as the most promising for further experiments.

We have determined whether HA could modulate complement activation when added in the formulations. This was done by the evaluation of protein C3 activation. This protein of the complement cascade is activated whatever the route of initiation of the activation of the complement system. Activation of the protein C3 is a good indicator on the capacity of macrophages of the MPS to phagocytose the drug carrier. Despite an increase of complement activation for the ratios 4 and 6 formulated with HA-DOPE compared to lipoplexes formulated without the conjugate, all formulations are low activators of the complement system, the formulation prepared at a lipids:DNA ratio of 2 being the less activating one. These data are in accordance with those of Mizrahy et al. reporting that unilamellar liposomes of 100 nm, containing 1500 kDa HA and composed of PC:Chol:DPPE slightly enhance complement activation [25]. This slight increase of complement activation in the presence of HA-DOPE could be due to polysaccharidic nature of HA, even if it is the lowest activator of glycosaminoglycans [26]. Another explanation could involve the way HA-DOPE is inserted in the lipid bilayer. Because more than one DOPE is linked on one chain of HA, the conjugate insertion could be obtained by more than one anchor, inducing the formation of a

specific conformation of the HA around the lipoplexes which might be different from the classic brush or mushroom. In any case, our goal to obtain lipoplexes with a low activating profile was reached. This is further supported by observations by Plank et al. [27] showing the low complement activation potential of the cationic lipids used. Finally, it is noteworthy that the lipoplex surface area used in this experiment was more than four times higher than what could be present after administration *in vivo* in a mouse model.

Transfection experiments were carried out on the A549 cancer cell line, which was shown in our hands to be a suitable model for targeting DNA because the totality of the cell population exhibits the CD44 membrane receptor [28]. Transfection efficiency of lipoplexes at different lipids:DNA ratios was tested at equivalent amount of intact DNA and using GFP plasmid as reporter gene. The optimal lipoplex formulation was the one containing 10% HA-DOPE at a lipids:DNA ratio of 2, which displayed a higher efficiency than lipoplexes without HA-DOPE, lipoplexes associated to unconjugated HA, and Lipofectin®. Moreover, when increasing the amount of HA-DOPE conjugate from 10 to 15%, the GFP expression dropped down to levels obtained with lipoplexes made without HA-DOPE. At this concentration, the amount of HA presented to cell might be too high to allow interaction with the CD44 receptor because of steric hindrance. These observations are supported by mechanistic studies demonstrating that when saturating CD44 receptor by an excess of HA or the CD44 epitope deadlock by antibody treatment, a strong reduction of GFP expression was observed. This also confirms the crucial role of the receptor in the endocytosis mediated process, as shown previously by us and others [25] and [29].

The more efficient formulation obtained at a lipids:DNA ratio of 2 with an amount of 10% HA was further characterized. Capillary electrophoresis was first used to indirectly quantify the amount of HA bound to the vesicles in the unconjugated form or conjugated to DOPE. The determination of the free fraction of HA compared to the total amount of HA added in formulations of ratio 2 shows that HA-DOPE binds to a lower extent to liposomes but strongly to lipoplexes as compared to liposomes/lipoplexes prepared with unconjugated HA. The use of HA-DOPE conjugate provides twice more association of HA to lipoplexes which could also explain the highest transfection efficiency of HA-DOPE containing lipoplexes. The presence of the anionic HA (conjugated or unconjugated) at the surface of cationic liposomes lowers the zeta potential values, demonstrating surface coverage. This external location is a prerequisite to confer cell specific targeting. We observed drastic size reduction when adding DNA to plain liposomes or liposomes containing HA-DOPE from values of around 400 nm down to 250 nm. Surprisingly, size reduction could not be observed with unconjugated HA. DNA that is negatively charged competes more efficiently with free negatively

charged HA that is bound only electrostatically to cationic liposomes. Whereas when HA is associated to lipid bilayer through its DOPE moiety insertion, competition between HA and DNA is lower: HA-DOPE does not interfere with lipoplex formation since it interacts mainly with liposomes by hydrophobic forces. Moreover, unconjugated HA inhibits lipoplex formation since HA is added before DNA in the process of lipoplex formation. This might explain why zeta potential values are more negative with lipoplexes containing unconjugated HA than with those containing HA-DOPE.

The endocytosis pathways were finally explored by different endocytosis-interfering treatments. There was no inhibitory effect of chlorpromazine, a cationic amphiphilic drug, which causes the loss of coated pits from the surface of the cell and blocks the appearance of clathrin coats on endosomal membranes [30]. This excludes clathrin-mediated endocytosis from being the pathway considered for the internalization of HA-DOPE-bearing lipoplexes. Since the perturbation of the caveolae, that is rich in cholesterol, by filipin, a sterol binding agent or by genistein, a kinase inhibitor [31] induces a decrease of the GFP expression in A549 cells, caveolae appear as the main endocytosis pathway of HA-bearing lipoplexes. Moreover, when CD44 is neutralized, transfection is also lowered suggesting that this receptor plays a role in lipoplex uptake. Caveolin-mediated endocytosis was already shown to be activated in the case of HA interaction with CD44 [32], both caveolin [33] and CD44 [34] being present in lipid rafts domains. Inhibition of CD44 by an excess of HA or CD44 antibody are known to block one of the pathways for caveolin phosphorylation which is necessary to start the caveolae-dependent endocytosis [32]. The reason why filipin and genistein are able to decrease in a larger manner the transfection level might be due to a higher inhibition of the caveolae-dependent endocytosis by cholesterol sequestration or perturbation of both dynamin and actin networks respectively, contrary to the inhibition of CD44 that impacts only a part of the caveolae process activation. Use of methylbetacyclodextrin in order to extract cholesterol was not possible as we observe cell dysmorphology and conclude to too much cytotoxicity on A549 whatever the concentration used. In A549 cells, clathrin-mediated endocytosis gives maximal levels of gene expression after an incubation period of 15 min, while maximal levels are being attained after 3 h for caveolae pathway [35]. The slow kinetics of GFP expression that we observed were typical for a caveolae-mediated internalization [35]. This caveolae mediated endocytosis is consistent with the internalization pathway of DMRIE:cholesterol (1:1) lipoplexes [36], but not with DOTAP lipoplexes that are internalized in A549 mainly by clathrin-mediated endocytosis [35]. Moreover our results are in accordance with others that show the ability of HA-bearing liposomes to interact with cells expressing CD44 [25] and [29].

Finally, the uptake and intracellular trafficking studies of fluorescent lipoplexes confirmed a progressive internalization associated with the formation of endosomes. The diffuse cytoplasmic fluorescence observed from 6 h indicates that lipoplexes are able to escape endosomes and reach the cytosol. Noteworthy, the plateau-like pattern from 6 h and the fraction of cells exhibiting intense diffuse cytoplasmic fluorescence is consistent with the transfection kinetics and fraction of cells transfected.

The DE-based, HA-bearing lipoplexes based on HA-DOPE, which display an interesting stability in serum-containing media, are thus promising for further *in vivo* evaluation using an anticancer therapeutic gene.

5. Conclusion

Among the different ratios tested, one formulation has notably emerged from transfection screening: lipoplexes prepared at a lipids:DNA ratio of 2 containing 10% HA-DOPE. This HA-DOPE incorporation rate leads to the most efficient formulation while maintaining a low complement activation. Here we provide additional information showing the interest of lipoplexes containing an HA-DOPE conjugate, which confers affinity to HA and allows a lipid bilayer insertion. Secondly, HA-DOPE is of interest because of the higher amount of HA associated to lipoplexes. And finally, this conjugate improves the transfection efficiency obtained after internalization that could be mediated by the CD44 receptor. This last point confers an ability of being internalized by cells expressing the CD44 membrane receptor, which may have a high potential to target tumor-initiatic cells.

Supplementary

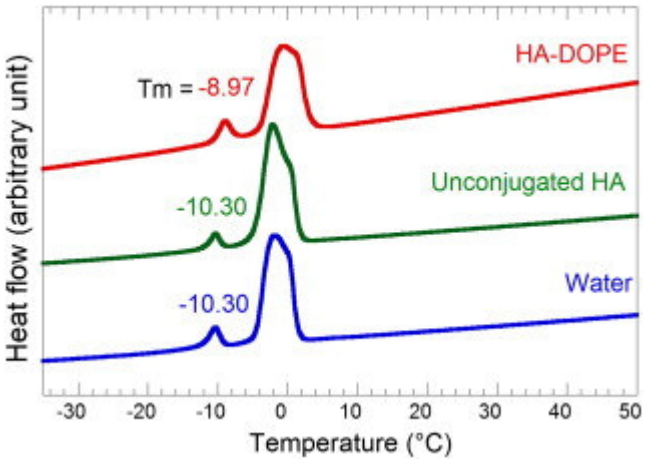

Figure S1.

Study of the transition temperature from gel to liquid crystalline phase of DOPE hydrated by different solutions (HA-DOPE, unconjugated HA and water) by differential scanning calorimetry. The first peak of each thermogram corresponds to the transition temperature (T_m) of hydrated DOPE and the second to the water melting. The three curves correspond (from top to bottom) to DOPE film hydrated by an aqueous solution of HA-DOPE 10%, DOPE film hydrated by an aqueous solution of unconjugated HA 10% and to DOPE film hydrated by water.

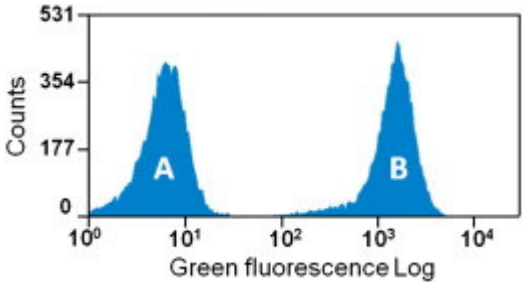

Figure S2.

A549 were stained with IgG1-labeled FITC antibody (A) and CD44-labeled FITC antibody (B). Each sample was measured in duplicate (10,000 cells measured per aliquot).

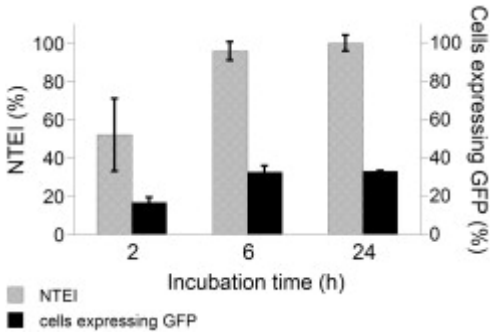

Figure S3.

A549 transfection kinetics of ratio lipids:DNA 2 containing 10% of HA-DOPE incubated for 2, 6 or 24 h. Flow cytometry results of normalized transfection efficacy index (NTEI) are expressed as the percentage of GFP-expressing cells and as the percentage of the NTEI reached at 24 h (*** $p < 0.001$; n = 3).

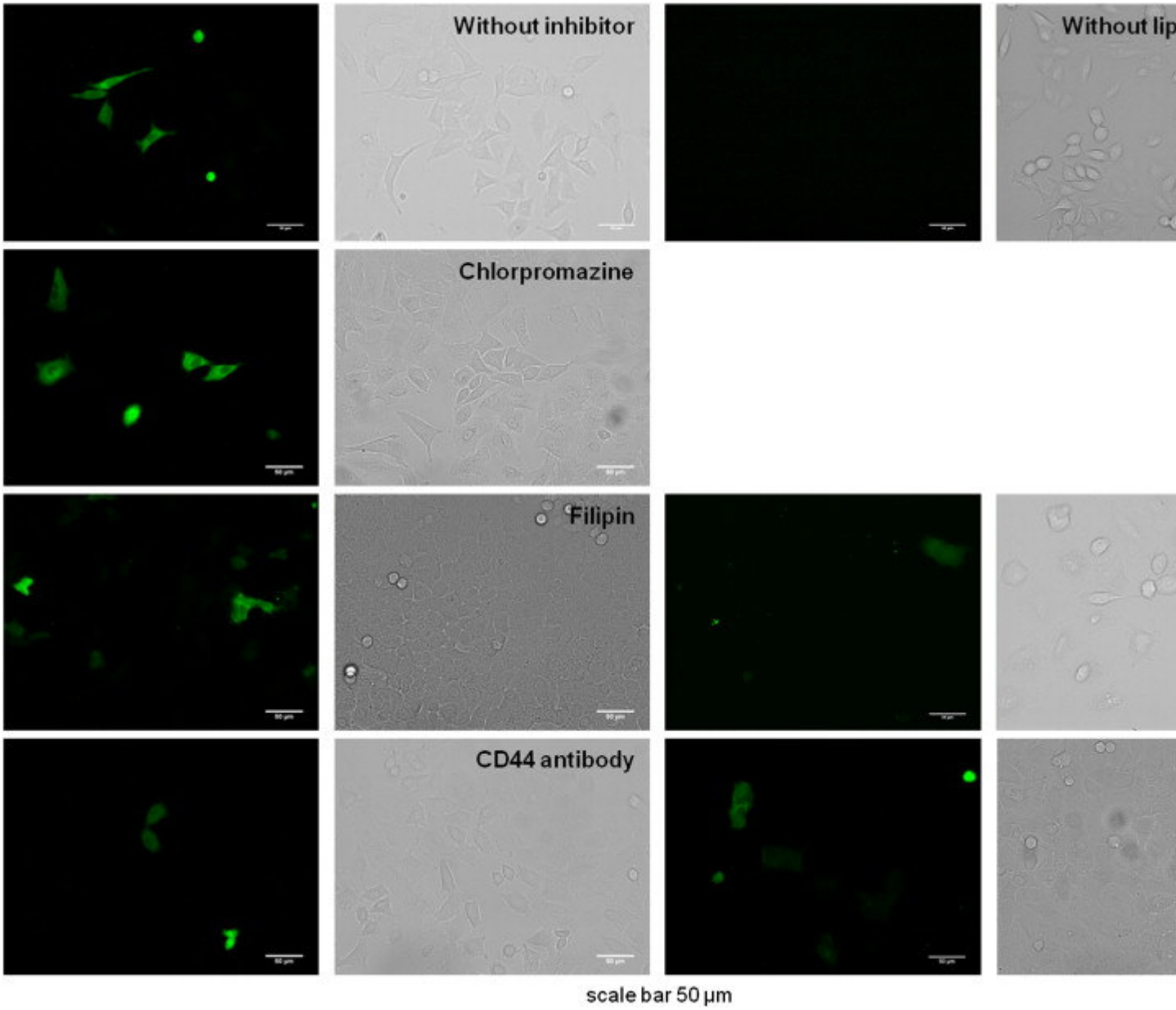

Figure S4.

Fluorescence and bright field images of A549 cells all treated by lipoplexes at lipids:DNA ratios of 2 containing 10% HA-DOPE (except negative control called “without lipoplexes or inhibitors”), after different endocytosis-interfering treatments: chlorpromazine, filipin, genistein, CD44 antibody, excess of HA.

Figure S5.

Three-dimensional reconstructions after surface rendering of confocal laser scanning microscopy slices corresponding to ‘m’ and ‘M’ cells shown in Fig. 9, after 2 h, 6 h and 24 h incubation with fluorescent lipoplexes.

Acknowledgments

This work has benefited from the facilities and expertise of the Imagif Cell Biology Unit of the Gif campus (www.imagif.cnrs.fr) which is supported by the Conseil Général de l'Essonne. We would like to acknowledge Marie Sophie Noël-Hudson for useful advices.

References

[1] C. Tros de Ilarduya, Y. Sun, N. Düzgüneş Gene delivery by lipoplexes and polyplexes Eur. J. Pharm. Sci., 40 (2010), pp. 159–170

[2] Y. Liu, D. Liggitt, W. Zhong, G. Tu, K. Gaensler, R. Debs Cationic liposome-mediated intravenous gene delivery J. Biol. Chem., 270 (1995), pp. 24864–24870

[3] M.J. Stewart, G.E. Plautz, L. Del Buono, Z.Y. Yang, L. Xu, X. Gao, L. Huang, E.G. Nabel, G.J. Nabel Gene transfer in vivo with DNA–liposome complexes: safety and acute toxicity in mice Hum. Gene Ther., 3 (1992), pp. 267–275

[4] N. Zhu, D. Liggitt, Y. Liu, R. Debs Systemic gene expression after intravenous DNA delivery into adult mice Science, 261 (1993), pp. 209–211

[5] Y. Yang, F.A. Nunes, K. Berencsi, E.E. Furth, E. Gonczol, J.M. Wilson Cellular immunity to viral antigens limits E1-deleted adenoviruses for gene therapy Proc. Natl. Acad. Sci. U. S. A., 91 (1994), pp. 4407–4411

[6] M.R. Knowles, K.W. Hohneker, Z. Zhou, J.C. Olsen, T.L. Noah, P.C. Hu, M.W. Leigh, J.F. Engelhardt, L.J. Edwards, K.R. Jones, M. Grossman, J.M. Wilson, L.G. Johnson, R.C. Boucher A controlled study of adenoviral-vector-mediated gene transfer in the nasal epithelium of patients with cystic fibrosis N. Engl. J. Med., 333 (1995), pp. 823–831

[7] A.R. Thierry, Y. Lunardi-Iskandar, J.L. Bryant, P. Rabinovich, R.C. Gallo, L.C. Mahan Systemic gene therapy: biodistribution and long-term expression of a transgene in mice Proc. Natl. Acad. Sci. U. S. A., 92 (1995), pp. 9742–9746

[8] R.I. Mahato, K. Kawabata, T. Nomura, Y. Takakura, M. Hashida Physicochemical and pharmacokinetic characteristics of plasmid DNA/cationic liposome complexes J. Pharm. Sci., 84 (1995), pp. 1267–1271

[9] M.B. Bally, P. Harvie, F.M. Wong, S. Kong, E.K. Wasan, D.L. Reimer Biological barriers to cellular delivery of lipid-based DNA carriers Adv. Drug Deliv. Rev., 38 (1999), pp. 291–315

[10] F. Shi, L. Wasungu, A. Nomden, M.C. Stuart, E. Polushkin, J.B. Engberts, D. Hoekstra Interference of poly(ethylene glycol)-lipid analogues with cationic-lipid-mediated delivery of oligonucleotides; role of lipid exchangeability and non-lamellar transitions Biochem. J., 366 (2002), pp. 333–341

[11] S.C. Semple, T.O. Harasym, K.A. Clow, S.M. Ansell, S.K. Klimuk, M.J. Hope Immunogenicity and rapid blood clearance of liposomes containing polyethylene glycol-lipid conjugates and nucleic Acid J. Pharmacol. Exp. Ther., 312 (2005), pp. 1020–1026

[12] P.W. Noble Hyaluronan and its catabolic products in tissue injury and repair Matrix Biol., 21 (2002), pp. 25–29

[13] R. Deed, P. Rooney, P. Kumar, J.D. Norton, J. Smith, A.J. Freemont, S. Kumar Early-response gene signalling is induced by angiogenic oligosaccharides of hyaluronan in endothelial cells. Inhibition by non-angiogenic, high-molecular-weight hyaluronan Int. J. Cancer, 71 (1997), pp. 251–256

[14] E.L. Pardue, S. Ibrahim, A. Ramamurthi Role of hyaluronan in angiogenesis and its utility to angiogenic tissue engineering Organogenesis, 4 (2008), pp. 203–214

[15] D. Peer, R. Margalit Loading mitomycin C inside long circulating hyaluronan targeted nano-liposomes increases its antitumor activity in three mice tumor models Int. J. Cancer, 108 (2004), pp. 780–789

[16] D. Peer, R. Margalit Tumor-targeted hyaluronan nanoliposomes increase the antitumor activity of liposomal Doxorubicin in syngeneic and human xenograft mouse tumor models Neoplasia, 6 (2004), pp. 343–353

[17] C. Surace, S. Arpicco, A. Dufay-Wojcicki, V. Marsaud, C. Bouclier, D. Clay, L. Cattel, J.M. Renoir, E. Fattal Lipoplexes targeting the CD44 hyaluronic acid receptor for efficient transfection of breast cancer cells Mol. Pharm., 6 (2009), pp. 1062–1073

[18] M. Al-Hajj, M.S. Wicha, A. Benito-Hernandez, S.J. Morrison, M.F. Clarke Prospective identification of tumorigenic breast cancer cells Proc. Natl. Acad. Sci. U. S. A., 100 (2003), pp. 3983–3988

[19] S. Arpicco, S. Canevari, M. Ceruti, E. Galmozzi, F. Rocco, L. Cattel Synthesis, characterization and transfection activity of new saturated and unsaturated cationic lipids Il Farmaco, 59 (2004), pp. 869–878

[20] J. Grimshaw, J. Trocha-Grimshaw, W. Fisher, A. Rice, S. Smith, P. Spedding, J. Duffy, R. Mollan Quantitative analysis of hyaluronan in human synovial fluid using capillary electrophoresis Electrophoresis, 17 (1996), pp. 396–400

[21] R. Diaz-Lopez, N. Tsapis, M. Santin, S. Bridal, V. Nicolas, D. Jaillard, D. Libong, P. Chaminade, V. Marsaud, C. Vauthier, E. Fattal The performance of PEGylated nanocapsules of perfluorooctyl bromide as an ultrasound contrast agent Biomaterials (2010), pp. 1723–1731

[22] M. Kazatchkine, G. Hauptmann, U. Nydegger Techniques du complement INSERM, Paris (1986)

[23] S.J. Eastman, C. Siegel, J. Tousignant, A.E. Smith, S.H. Cheng, R.K. Scheule Biophysical characterization of cationic lipid: DNA complexes Biochim. Biophys. Acta, 1325 (1997), pp. 41–62

[24] O. Zelphati, L.S. Uyechi, L.G. Barron, F.C. Szoka Jr. Effect of serum components on the physico-chemical properties of cationic lipid/oligonucleotide complexes and on their interactions with cells Biochim. Biophys. Acta, 1390 (1998), pp. 119–133

[25] S. Mizrahy, S.R. Raz, M. Hasgaard, H. Liu, N. Soffer-Tsur, K. Cohen, R. Dvash, D. Landsman-Milo, M.G.E.G. Bremer, S.M. Moghimi, D. Peer Hyaluronan-coated nanoparticles: the influence of the molecular weight on CD44-hyaluronan interactions and on the immune response J. Control. Release, 156 (2011), pp. 231–238

[26] N.S. Chang, R.J. Boackle Glycosaminoglycans enhance complement hemolytic efficiency: theoretical considerations for GAG-complement-saliva interactions Mol. Immunol., 23 (1986), pp. 887–893

[27] C. Plank, K. Mechtler, F.C. Szoka Jr., E. Wagner Activation of the complement system by synthetic DNA complexes: a potential barrier for intravenous gene delivery Hum. Gene Ther., 7 (1996), pp. 1437–1446

[28] S. Taetz, A. Bochot, C. Surace, S. Arpicco, J.M. Renoir, U.F. Schaefer, V. Marsaud, S. Kerdine-Roemer, C.M. Lehr, E. Fattal Hyaluronic acid-modified DOTAP/DOPE liposomes for the targeted delivery of anti-telomerase siRNA to CD44-expressing lung cancer cells Oligonucleotides, 19 (2009), pp. 103–115

[29] H.S.S. Qhattal, X. Liu Characterization of CD44-mediated cancer cell uptake and intracellular distribution of hyaluronan-grafted liposomes Mol. Pharm., 8 (2011), pp. 1233–1246

[30] L.H. Wang, K.G. Rothberg, R.G. Anderson Mis-assembly of clathrin lattices on endosomes reveals a regulatory switch for coated pit formation J. Cell Biol., 123 (1993), pp. 1107–1117

[31] J.E. Schnitzer, P. Oh, E. Pinney, J. Allard Filipin-sensitive caveolae-mediated transport in endothelium: reduced transcytosis, scavenger endocytosis, and capillary permeability of select macromolecules J. Cell Biol., 127 (1994), pp. 1217–1232

[32] M. Long, S.-H. Huang, C.-H. Wu, G. Shackleford, A. Jong Lipid raft/caveolae signaling is required for *Cryptococcus neoformans* invasion into human brain microvascular endothelial cells J. Biomed. Sci., 19 (2012), p. 19

[33] N.M. Hooper Detergent-insoluble glycosphingolipid/cholesterol-rich membrane domains, lipid rafts and caveolae Mol. Membr. Biol., 16 (1999), pp. 145–156

[34] H. Ponta, L. Sherman, P.A. Herrlich CD44: from adhesion molecules to signalling regulators Nat. Rev. Mol. Cell Biol., 4 (2003), pp. 33–45

[35] J. Rejman, A. Bragonzi, M. Conese Role of clathrin- and caveolae-mediated endocytosis in gene transfer mediated by lipo- and polyplexes Mol. Ther., 12 (2005), pp. 468–474

[36] A.W. Wong, S.J. Scales, D.E. Reilly DNA internalized via caveolae requires microtubule-dependent, Rab7-independent transport to the late endocytic pathway for delivery to the nucleusJ. Biol. Chem., 282 (2007), pp. 22953–22963